

available at [www.sciencedirect.com](http://www.sciencedirect.com)journal homepage: [www.elsevier.com/locate/carbon](http://www.elsevier.com/locate/carbon)

# Graphite nanoplatelet pastes vs. carbon black pastes as thermal interface materials

Chuangang Lin, D.D.L. Chung\*

Composite Materials Research Laboratory, University at Buffalo, State University of New York, Buffalo, NY 14260-4400, USA

## ARTICLE INFO

### Article history:

Received 11 March 2008

Accepted 9 October 2008

Available online 17 October 2008

## ABSTRACT

Comparison of graphite nanoplatelet (GNP) and carbon black (CB) pastes as thermal interface materials shows that the optimum filler content for attaining the maximum thermal contact conductance (copper proximate surfaces, roughness 15  $\mu\text{m}$ ) are 2.4, 15 and 2.4 vol.% for GNP, CB (Tokai) and CB (Cabot), respectively. Except for CB (Cabot), the optimum filler content is diminished when the roughness is decreased from 15 to 0.009  $\mu\text{m}$ . Comparing the fillers at their respective optimum contents shows that (i) GNP is similarly effective as CB (Tokai) for rough (15  $\mu\text{m}$ ) surfaces, but is less effective than CB (Tokai) for smooth (0.009  $\mu\text{m}$ ) surfaces, and (ii) GNP is more effective than CB (Cabot) for rough surfaces, but is slightly less effective than CB (Cabot) for smooth surfaces. GNP gives higher thermal conductivity and greater bond line thickness than CB (Tokai or Cabot), whether the comparison is at the same filler content or at the respective optimum filler contents. In spite of the high thermal conductivity, the effectiveness of GNP is limited, due to the high bond line thickness. CB (Tokai) gives higher thermal conductivity than CB (Cabot), thus causing CB (Tokai) to be more effective than CB (Cabot).

© 2008 Elsevier Ltd. All rights reserved.

## 1. Introduction

Thermal interface pastes are needed for improving thermal contacts, which are critical to the cooling of microelectronics. An example of a thermal contact is the interface between the microprocessor and the heat sink of a computer.

A thermal paste comprises an organic vehicle and a solid component that is thermally conductive. The solid component is typically in the form of fine particles that are dispersed and suspended in the vehicle.

A high value of the thermal conductivity does not imply that the material will be an effective thermal interface material. This is because the thermal conductivity is only one of the factors that affect the performance of a thermal interface material. Other factors are the conformability and the spreadability. Even if the interface material may be an excellent thermal conductor, poor conformability would make it ineffective

as a thermal interface material. Spreadability refers to the ability for the interface material to become very thin at the interface. This factor is also important, because the thermal resistance due to the interface material increases with the thickness of the interface material.

Carbon black provides thermal pastes that are superior to commercial silver paste (Arctic Silver Inc., Visalia, CA), commercial ceramic paste (Arctic Silver Inc.), carbon nanotube pastes and solder [1–9]. In spite of the high thermal conductivity of the commercial silver paste and the low thermal conductivity of carbon black, the carbon black paste is more effective [2,3,6]. This fact points to the importance of conformability, which is poor for the commercial silver paste. Due to its conformability, the carbon black thermal paste is more effective than commercial thermal pastes that contain silver particles or boron nitride particles of high thermal conductivity when the proximate surfaces of the thermal contact

\* Corresponding author. Fax: +1 716 645 2883.

E-mail address: [ddlchung@buffalo.edu](mailto:ddlchung@buffalo.edu) (D.D.L. Chung).

URL: <http://alum.mit.edu/www/ddlchung> (D.D.L. Chung).

0008-6223/\$ - see front matter © 2008 Elsevier Ltd. All rights reserved.

doi:10.1016/j.carbon.2008.10.011

are sufficiently smooth (e.g., a roughness of  $0.009\text{ }\mu\text{m}$  [5]). The rougher are the proximate surfaces, the more important is the thermal conductivity within the paste. As a result, the superior performance of the carbon black paste occurs only when the proximate surfaces are smooth enough.

Exfoliated graphite is a form of graphite that is made by intercalation, followed by exfoliation, which is commonly conducted by heating at a high temperature [10]. Exfoliation is accompanied by extensive expansion in the direction perpendicular to the graphite atomic planes. Microscopically, the exfoliation process involves the opening up of the graphite structure like an accordion. Mechanical agitation (such as sonication) carried out on exfoliated graphite tends to break up the material into nanoplatelets [11], which are attractive for making polymer-matrix nanocomposites, in which the nanoplatelets serve as a reinforcement [12–15] and/or a conductive filler [16–19]. Graphite nanoplatelets (GNP) are less expensive than carbon nanotubes, but they are more expensive than carbon black.

Yu et al. [20] recently reported that GNP is an effective filler for a thermal interface material in the form of an epoxy-matrix composite. However, this statement is not supported by the research results of Yu et al., as explained below. Evaluation of the effectiveness of a thermal interface material requires measurement of the thermal resistance associated with the sandwich that consists of the two proximate surfaces and the interface material between them. Such a measurement is absent in the work of Yu et al.

Flexible graphite (sheet formed by compressing exfoliated graphite without a binder; often known by the tradename “Grafoil”) is also a thermal interface material [21]. In spite of its resilience in the direction perpendicular to the sheet, flexible graphite by itself is not highly effective as a thermal interface material [21]. Nevertheless, flexible graphite is effective as a carrier (substrate) for thermal pastes for providing thermal gap-filling materials [5]. On the other hand, aluminum foil is also effective as a carrier [5].

A large aspect ratio of the graphite nanoplatelets is advantageous for the thermal conductivity within the composite, as recognized by Yu et al. [20]. However, it may possibly be a disadvantage for thermal interface material performance. This is because of the tendency for the nanoplatelets to orient preferentially in the plane of the thermal interface. The thermal conductivity of a nanoplatelet is relatively poor in the direction perpendicular to the plane of the nanoplatelet. Carbon nanotubes have a similar problem, due to their tendency to orient in the plane of the thermal interface. Alignment of the graphite nanoplatelets or carbon nanotubes is possible, but it adds to the cost and limits the applicability. For example, aligned nanotube arrays can be grown by chemical vapor deposition on silicon substrates [22,23]. In contrast, the carbon black particles are essentially spherical in shape. In spite of the relatively high value of the thermal conductivity of the carbon nanotube array [23], the large bond line thickness of  $0.1\text{ mm}$  (or above) limits the effectiveness of the array as a thermal interface material.

The relatively large size ( $0.35\text{--}1.7\text{ }\mu\text{m}$ ) of a graphite nanoplatelet in the plane of the nanoplatelet [20] is another possible disadvantage for thermal interface material performance. This large size is expected to limit the conformability, as the

valleys in the surface topography of the proximate surfaces can be as small as nanometers in size. Carbon nanotubes have a similar problem, due to their relatively large size along the axis of the nanotube. In contrast, the carbon black particles are small, around  $30\text{ nm}$  in size.

The conformability of a thermal interface material depends on both the filler and the matrix. A stiff matrix will not allow the composite material to conform. The matrix used by Yu et al. [20] is epoxy that has been cured completely. As a consequence, the composites of Yu et al. are stiff and not conformable. The low conformability will result in poor performance as a thermal interface material. In contrast, the carbon black pastes involve soft matrices [1–9].

Yu et al. [20] stated that the thermal conductivity attained in their work surpasses the performance of conventional fillers that require a loading of  $\sim 70\text{ vol.}\%$  to achieve these values. This statement is not accurate. The highest value of the thermal conductivity attained by Yu et al. is  $6.44\text{ W/mK}$ . This value is low compared to  $11.0\text{ W/mK}$  for epoxy containing  $60\text{ vol.}\%$  aluminum nitride particles and  $10.3\text{ W/mK}$  for epoxy containing  $57\text{ vol.}\%$  boron nitride particles [24].

Due to the various problematic issues mentioned above concerning the report of Yu et al. [20], this paper is aimed at (i) evaluating the performance of GNP thermal pastes by measurement of the thermal contact conductance across a sandwich consisting of proximate surfaces with the paste in between – a measurement that is missing in the work of Yu et al., and (ii) comparing the performance of GNP pastes with that of carbon black pastes with the same vehicle (a soft matrix, in contrast to the stiff matrix used by Yu et al.).

## 2. Experimental

### 2.1. Materials

The as-received graphite intercalation compound flake (GIC, flake graphite intercalated by sulfuric acid and nitric acid in the presence of catalysts, with a flake size of  $300\text{ }\mu\text{m}$ , as supplied by Asbury Graphite Mills, Asbury, NJ) was heated in a furnace at  $1000\text{ }^{\circ}\text{C}$  in purging nitrogen for 2 min for the purpose of exfoliation to form expanded (or exfoliated) graphite (abbreviated EG). The expanded graphite obtained was then immersed in acetone and sonicated using an ultrasonicator (Fisher Scientific International Inc, FS60H, Hampton, NH) at  $100\text{ W}$  for 24 h in order to obtain GNP dispersions at a concentration of  $2\text{ mg/ml}$ .

GNP pastes were prepared using the following steps. A polyol ester oil (Hatcol 2372, Hatco Corp., Fords, NJ) was added to a GNP/acetone suspension, which was then subjected to 5 min of hand mixing. A large portion of the acetone was then removed by evaporation using a hot plate held at  $100\text{ }^{\circ}\text{C}$  for 2 h. Any remaining acetone was then removed by placing the sample in a vacuum chamber and heating to  $85\text{ }^{\circ}\text{C}$  for 24 h. Polyol-ester-based pastes containing 0.6, 1.2, 2.4, 3.6 and  $4.8\text{ vol.}\%$  GNP were studied.

For the sake of comparison, polyol ester pastes containing carbon black (CB) were also studied. Two types of CB were used, namely Vulcan XC72R (Cabot Corp., Billerica, MA) and Tokaiblack #3800 (graphitized carbon black from Tokai Carbon Co., Ltd., Tokyo, Japan).

## 2.2. Testing

### 2.2.1. Thermal contact conductance measurement

A steady-state method known as the guarded hot plate method (ASTM Method D5470) was used to measure the thermal contact conductance of thermal contacts that utilized various thermal pastes at the thermal interface. Various thermal pastes were sandwiched between the 1 × 1 inch (25 × 25 mm) proximate surfaces of two copper blocks (both 1 × 1 inch surfaces of each block having a controlled degree of roughness). Each copper block had a height of 35 mm. The two proximate surfaces of the two 1 × 1 in copper blocks were either “rough” (15 μm roughness, as attained by mechanical polishing) or “smooth” (0.009 μm roughness and 0.040–0.116 μm flatness, as attained by diamond turning). A pressure of 0.46, 0.69 or 0.92 MPa was applied in the direction perpendicular to the thermal interface during the measurement. The testing method is as described in prior publications by Chung et al. [7,8].

### 2.2.2. Thermal conductivity measurement

The thermal conductivity within a thermal paste is to be distinguished from the thermal contact conductance across a thermal contact. This thermal conductivity measurement was also based on the ASTM D5470 method, as explained below.

The thermal resistance of a system consisting of a thermal paste sandwiched by a heat source and a heat sink can be simply modeled by thermal resistances in series. Thus,

$$R = \frac{h}{kA} + R_1 + R_2 \quad (1)$$

where  $A$  is the geometric area of the contact,  $h$  is the bond line thickness,  $k$  is the thermal conductivity of the thermal paste,  $R$  (in unit of K/W) is the total thermal resistance of the sandwich, and  $R_1$  and  $R_2$  are the interfacial resistances of the interface between the thermal paste and the two surfaces that sandwich the paste [24]. The geometric area is the flat contact area and is to be distinguished from the true area, which reflects the interface area associated with the roughness of each of the proximate surfaces. The total thermal resistivity of the sandwich is  $RA$  (in unit of m<sup>2</sup>K/W). The inverse of the thermal resistivity is the thermal contact conductance (in unit of W/m<sup>2</sup>K).

The thermal conductivity  $k$  was determined by measuring the thermal resistivity  $RA$  for various values of the thermal paste thickness  $h$ . The plot of  $RA$  vs.  $h$  is linear, with slope  $1/k$ , and intercept  $(R_1 + R_2)A$  at the vertical axis, as indicated by Eq. (1) [25]. The product  $R_1A$  is the geometric interfacial resistivity of the interface between the thermal paste and one of the two proximate surfaces, while the product  $R_2A$  is the geometric interfacial resistivity of the interface between the thermal paste and the other proximate surface.

In order to control the bond line thickness of the thermal paste sandwiched by the two proximate surfaces, four stainless steel spacers [26] were used, as illustrated in Fig. 1. Each spacer was a short prism based on a 2 × 2 mm<sup>2</sup>. In order to control the thickness of the paste to be tested, four sets of spacers with different column heights were used, namely 50, 100, 150 and 200 μm. The proximate surfaces used for

thermal conductivity measurement had a roughness of 0.05 μm. This roughness is between those of the rough and smooth surfaces used in thermal contact conductance measurement (Section 2.2.1). A pressure of 0.25 MPa was applied in the direction perpendicular to the thermal interface during the measurement. The pressure was borne by the four spacers, while the thermal paste filled the space between the two proximate surfaces. In other words, the thermal paste was not under pressure during the thermal conductivity measurement; only the spacers were.

Due to the absence of pressure on the paste, the values of the thermal conductivity and the geometric interfacial resistivity determined by this method are for the unloaded state and are therefore different from the corresponding values in the thermal contact conductance measurement configuration, which involved application of pressure to the paste. Since pressure helps the conformability of the paste to the topography of the proximate surfaces, pressure is expected to decrease the geometric interfacial resistivity. As a result, the geometric interfacial resistivity determined by using this method must be higher than that for the thermal contact conductance measurement configuration. Furthermore, pressure is expected to affect the thermal conductivity of the paste, due to the effect of pressure on the preferred orientation of the GNP in the paste and on the degree of squishing of the carbon black in the paste.

The contribution of the spacers, which are high in thermal conductivity, to the overall thermal resistance of the sandwich was excluded in the calculation of the thermal conductivity of the thermal paste in the sandwich. The contribution of the spacers to the heat flow was determined by measuring the thermal contact conductance of the sandwich held by the spacers in the absence of a paste. Then the heat flow associated with the thermal paste was obtained by deducting the heat flow due to the spacers from the heat flow due to the combination of spacers and paste. Thus, the effect of the spacers on the determination of the thermal conductivity of the paste was eliminated.

### 2.2.3. Bond line thickness measurement

The bond line thickness (i.e., thermal paste thickness) of a thermal contact is an important parameter that affects performance. Measurement of the bond line thickness using a strain gage in conjunction with the set-up for thermal contact conductance is inaccurate when the thickness is below about 3 μm [27]. Therefore, this work used other methods, called Methods A and B, for bond line thickness measurement, as explained below.

Method A involved an indirect method, in which the bond line thickness was calculated from the controlled volume of the thermal paste and the measured area of the thermal paste after the spreading associated with its being sandwiched by the copper blocks (those used for thermal contact conductance measurement) at a controlled load (provided by a constant weight) for 1 min. The paste was applied to the center of the surface of one of the copper blocks prior to bringing the two blocks together and subsequent compression, which caused the paste to spread. After the compression, the blocks were separated and the diameter of the spread paste was measured. The area of the spread paste was calculated from

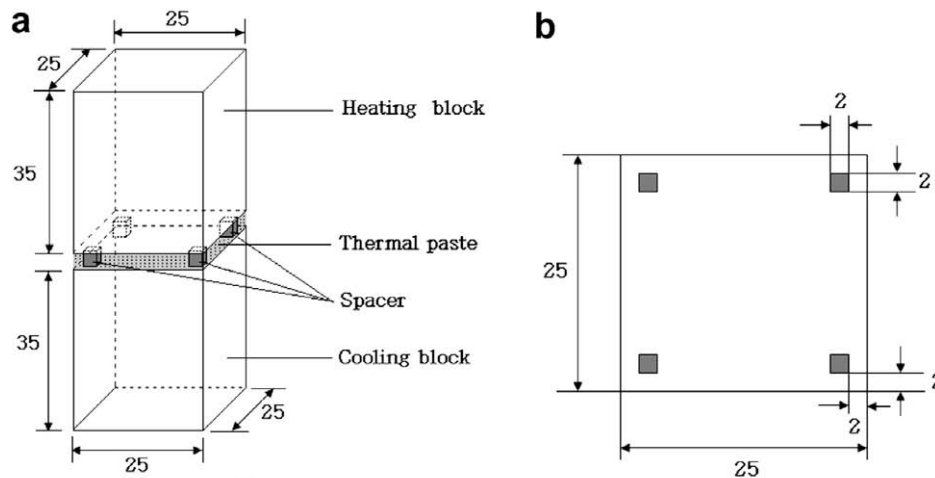


**Fig. 1 – Thermal conductivity measurement by using spacers to control the thermal paste thickness. All dimensions are in mm. (a) Three-dimensional view, with the height of each spacer much exaggerated. (b) Top view.**

the measured diameter of the spread paste, as the area was essentially circular. The pressure of the compression was calculated from the constant weight and the area covered by the spread paste. By using different volumes of thermal paste, hence different areas covered by the spread paste, the pressure on the paste was varied, thereby allowing investigation of the dependence of the bond line thickness on the pressure. The pressure range was similar to that used for thermal contact conductance measurement (Section 2.2.1).

Method B involved direct measurement of the bond line thickness as a function of time after application of a constant pressure that was considerably below the pressures used in thermal contact conductance measurement. That the pressure used in Method B was low is because of the upper limit in force that could be provided by the thermomechanical analyzer (TMA7, Perkin-Elmer Inc., Waltham, MA) used. This analyzer is attractive because it is capable of measuring dimensional changes with a displacement sensitivity of 50 nm and a resolution of 3 nm [28]. Although it allows temperature variation, this work used it only at room temperature. The low pressure makes Method B not as relevant as Method A, but Method B provides information on the change in bond line thickness as a function of time after pressure application.

In Method B, a controlled volume of the paste to be evaluated was applied to be interface between two copper discs of diameter 7 mm and roughness 15  $\mu\text{m}$ . A compressive load of only 30 mN (i.e., a stress of 780 Pa) was applied to the sandwich in the direction perpendicular to the thermal interface. The change of the bond line thickness immediately after the load application was monitored as a function of time by using the quartz position probe (with diameter 3 mm and a flat tip) associated with the thermomechanical analyzer.

#### 2.2.4. Microstructural examination

The microstructure of EG (prior to sonication) and of GNP (after sonication) was observed by using a scanning electron microscope (SEM) in the secondary electron imaging mode.

### 3. Results and discussion

#### 3.1. Microstructure of EG and GNP

Fig. 2a shows the worm-like shape of EG, while Fig. 2b, at a higher magnification, shows the accordion-like microstructure of EG. These shape and microstructure are typical of EG, as previously reported [17]. They are consistent with the well-known fact that exfoliation involved expansion by up to several hundred times along the thickness direction of the flake, due to vapor generation by the intercalate [10].

Fig. 2c and d show the nanoplatelet morphology of GNP at two magnifications. The platelets had dimensions around 3–8  $\mu\text{m}$  in the plane of a platelet. The platelet thickness was in the nanoscale.

#### 3.2. Thermal contact conductance

Table 1 and Fig. 3 show the thermal contact conductance of GNP pastes and CB pastes for both rough and smooth surfaces. For the case of rough surfaces, GNP was slightly more effective than CB (Tokai), which was in turn more effective than CB (Cabot). For the case of smooth surfaces, CB (Tokai) was more effective than CB (Cabot), which was in turn more effective than GNP. This comparison is based on the best performance among various filler volume fractions for each type of filler. The highest value of the thermal contact conductance attained in this work for the rough case is  $12 \times 10^4 \text{ W/m}^2 \text{ }^\circ\text{C}$  (as attained by GNP); the highest value of the conductance attained in this work for the smooth case is  $33 \times 10^4 \text{ W/m}^2 \text{ }^\circ\text{C}$  (as attained by CB (Tokai)).

The high effectiveness of GNP for the rough case is attributed to the high thermal conductivity of GNP (Section 3.3). The high effectiveness of CB (Tokai) for the smooth case is attributed to the high conformability that is suggested by the low viscosity [27]. Thermal conductivity is more important for rough surfaces than smooth surfaces, whereas

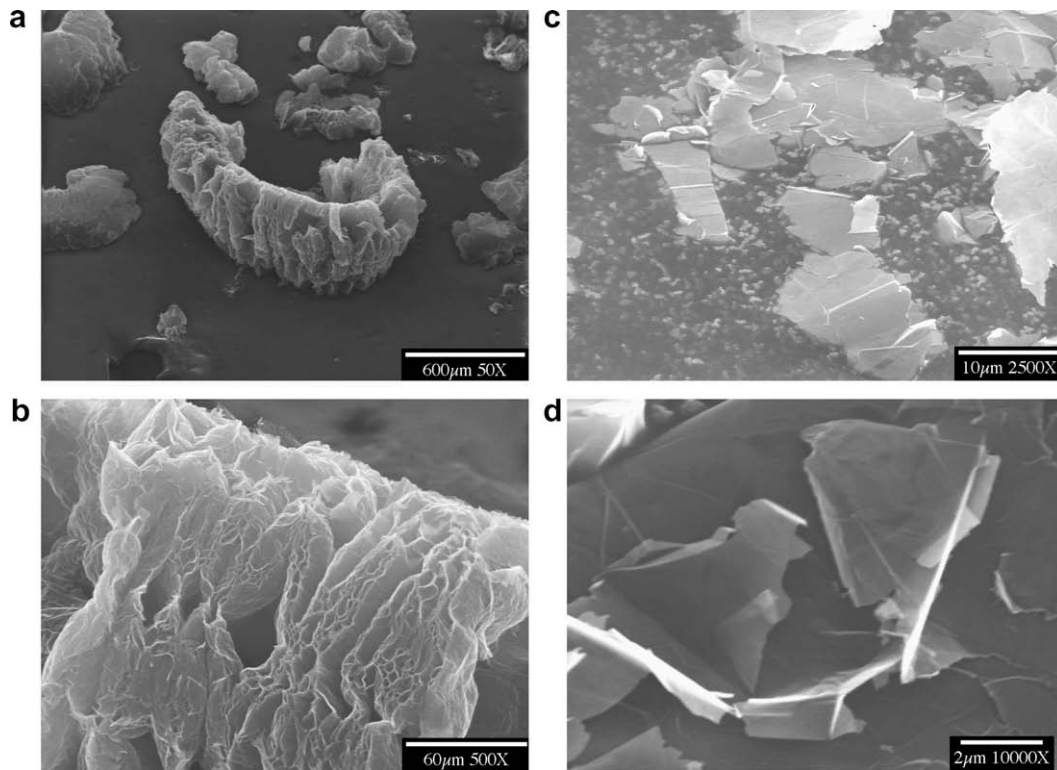


Fig. 2 – SEM photographs. (a) and (b) Exfoliated graphite before sonication. (c) and (d) Graphite nanoplatelets obtained by sonication of exfoliated graphite.

**Table 1 – Thermal contact conductance of thermal contacts with GNP pastes and carbon black (CB) pastes. The bond line thicknesses of various pastes are shown in Fig. 8.**

Thermal paste		Thermal conductance ( $10^4 \text{ W/m}^2\text{°C}$ )				
Filler	Vol.%	Rough surfaces			Smooth surfaces	
		0.46 MPa	0.69 MPa	0.92 MPa	0.46 MPa	0.69 MPa
GNP	0.6	/	/	/	$23.81 \pm 0.34$	$25.18 \pm 0.21$
	1.2	$10.66 \pm 0.04$	$11.38 \pm 0.05$	$11.66 \pm 0.06$	$24.26 \pm 0.66$	$25.66 \pm 0.06$
	2.4	$11.72 \pm 0.28$	$11.98 \pm 0.18$	$12.36 \pm 0.10$	$22.07 \pm 1.18$	$24.47 \pm 0.37$
	3.6	$10.32 \pm 0.15$	$10.71 \pm 0.05$	$11.17 \pm 0.09$	$21.17 \pm 0.07$	$22.16 \pm 0.28$
	4.8	$9.35 \pm 0.34$	$10.74 \pm 0.32$	$9.68 \pm 0.34$	$17.40 \pm 0.37$	$19.14 \pm 0.21$
CB (Tokai)	1.2	$9.45 \pm 0.02$	$9.59 \pm 0.09$	$9.89 \pm 0.02$	/	/
	2.4	$10.20 \pm 0.20$	$11.01 \pm 0.05$	$11.87 \pm 0.08$	$24.23 \pm 0.17$	$27.75 \pm 0.11$
	4.8	$10.12 \pm 0.16$	$11.10 \pm 0.10$	$11.59 \pm 0.15$	/	/
	8.0	$10.85 \pm 0.20$	$11.39 \pm 0.10$	$11.64 \pm 0.12$	$30.41 \pm 0.47$	$32.75 \pm 0.19$
	12.0	$11.06 \pm 0.27$	$11.71 \pm 0.12$	$12.57 \pm 0.28$	/	/
	15.0	$11.27 \pm 0.34$	$12.41 \pm 0.22$	$13.18 \pm 0.11$	$25.58 \pm 0.35$	$27.86 \pm 0.10$
	20.0	$9.34 \pm 0.21$	$9.86 \pm 0.11$	$11.11 \pm 0.13$	$17.48 \pm 0.17$	$22.33 \pm 0.29$
CB (Cabot)	1.2	$8.50 \pm 0.16$	$9.39 \pm 0.11$	$10.36 \pm 0.20$	/	/
	2.4	$8.72 \pm 0.07$	$10.18 \pm 0.20$	$11.12 \pm 0.12$	$25.91 \pm 0.16$	$27.75 \pm 0.14$
	4.8	$8.45 \pm 0.11$	$9.39 \pm 0.15$	$10.58 \pm 0.11$	$19.10 \pm 0.20$	$21.33 \pm 0.32$
	8.0	$7.96 \pm 0.08$	$8.71 \pm 0.10$	$8.78 \pm 0.09$	$16.52 \pm 0.61$	$18.17 \pm 0.22$
	12.0	$2.05 \pm 0.02$	$2.28 \pm 0.03$	$2.49 \pm 0.02$	/	/

conformability is more important for smooth surfaces than rough surfaces.

The optimum filler volume fraction differed among the three filler types. For the case of rough surfaces, the optimum was 2.4, 15 and 2.4 vol.% for GNP, CB (Tokai) and CB (Cabot),

respectively. For the case of smooth surfaces, the optimum was 1.2, 8 and 2.4 vol.% for GNP, CB (Tokai) and CB (Cabot), respectively. Thus, the optimum filler volume fraction was diminished by having smoother proximate surfaces for GNP and CB (Tokai), but was not affected by the smoothness for



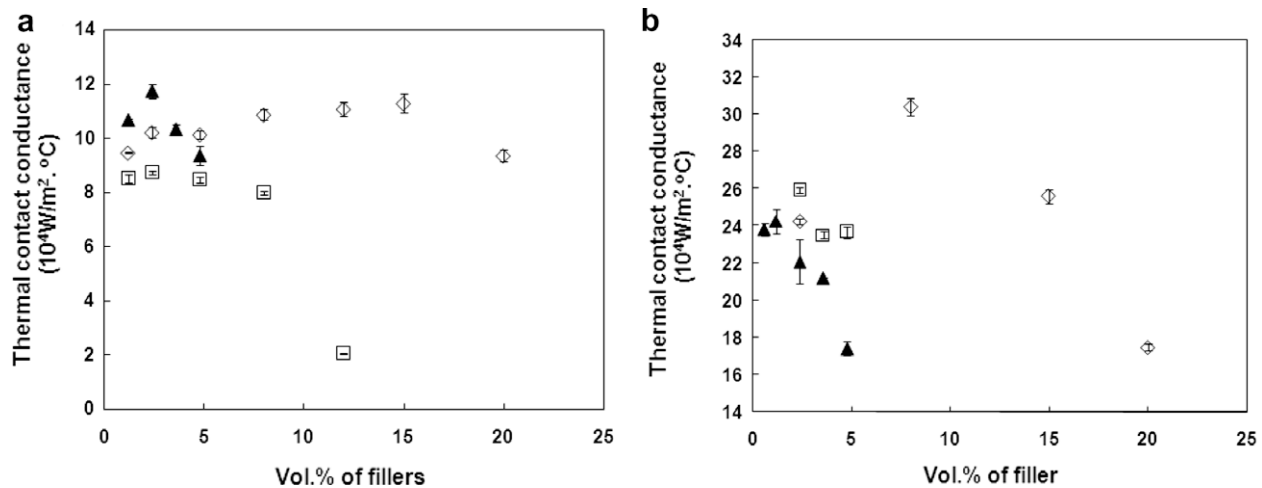


**Fig. 3 – Thermal contact conductance measured for the case of (a) rough surfaces, and (b) smooth surfaces. (▲) GNP; (◇) carbon black (Tokai); (□) carbon black (Cabot). A vertical bar with a horizontal line at each end and indicating the data scatter is shown for each data point, though the bar is negligibly short for most data points.**

CB (Cabot). For GNP beyond the optimum volume fraction, the conductance decreased significantly with increasing GNP volume fraction (Fig. 3). Due to the low value of the optimum filler volume fraction for GNP compared to CB (Tokai), GNP was less effective than CB (Tokai) when the filler volume fraction exceeded about 5 vol.% for the rough case. The existence of an optimum is due to the fact that the thermal conductivity of the paste increases with increasing filler content, while the conformability and spreadability of the paste decrease with increasing filler content. That the optimum volume fraction is higher for rough surfaces than smooth surfaces for the same filler type, as shown for both GNP and CB (Tokai), is due to the relatively high importance of the thermal conductivity for the rough case and the relatively high importance of the conformability for the smooth case. That the optimum volume fraction is higher for CB (Tokai) than CB (Cabot), as shown for both rough and smooth cases, and that CB (Tokai) is more effective than CB (Cabot), as shown for the rough case, are due to the lower DBP value (i.e., the lower structure) of CB (Tokai), as previously reported [27]. Although GNP is in the nanoscale in the thickness direction of the platelet, it is in the micrometer scale in the plane of the platelet. The large in-plane dimension and the expected tendency for the flakes to lie down in the plane of the thermal interface probably contribute to causing GNP to have a low optimum filler volume fraction, akin to CB (Cabot), in the rough case.

All values of the thermal contact conductance reported in this work (Table 1) are higher than the highest value of  $8 \times 10^3 \text{ W/m}^2 \text{ K}$  that had been previously reported for both an aligned multiwalled carbon nanotube (0.4 vol.%) array and a non-aligned dispersed multiwalled carbon nanotube (0.4 vol.%) silicone-matrix composite [23].

### 3.3. Thermal conductivity

Table 2 and Fig. 4 illustrate, for the case of the paste with 2.4 vol.% GNP, how the raw data were used, according to the method described in Section 2.2.2, to determine the thermal conductivity of a paste. Based on the linear equation associ-

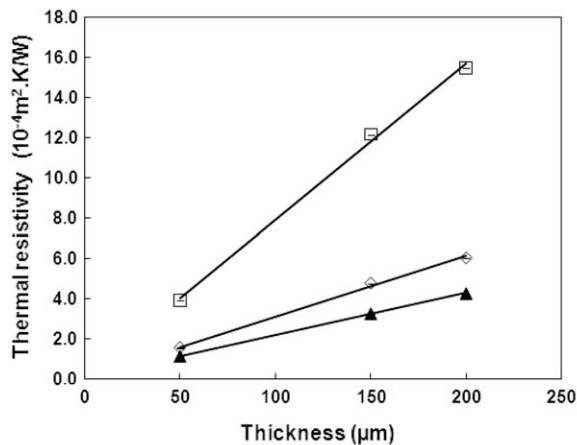
ated with the plot of the thermal resistivity (overall) vs. the paste thickness, the thermal conductivity  $k$  of the paste was determined for this paste to be  $1/2 \cdot 103 = 0.476 \text{ W/mK}$  and the total geometric interfacial resistivity of the two paste-copper interfaces in the sandwich was determined for this paste to be  $6.2 \times 10^{-6} \text{ m}^2 \text{ K/W}$ .

Table 3 shows the geometric interfacial resistivity for various pastes under no pressure. The values are comparable for GNP and CB pastes. Under pressure, the values are expected to be lower, since the pressure increases the conformability. In spite of the overestimation, the values of the geometric interfacial resistivity of all the pastes studied are of the order of  $10^{-5}$ – $10^{-6} \text{ m}^2 \text{ K/W}$  which is comparable to values previously reported for the interface between copper (of unspecified surface roughness) and an aligned carbon nanotube array [23]. Though the thermal conductivity of the array is  $1.21 \text{ W/mK}$ , which is higher than any of the thermal conductivity values of this work (Table 3), the array's high bond line thickness (0.1 mm or above) limits its effectiveness, which is shown by the low values of the thermal contact conductance mentioned in Section 3.2.

Table 3 and Fig. 5 show the thermal conductivity values obtained for the various pastes under no pressure. The values of the GNP paste thermal conductivity reported here are comparable to those previously reported for GNP filled epoxy at similar filler volume fractions [29]. GNP gives higher thermal conductivity than either type of CB, whether the comparison is at the same filler volume fraction or at the respective optimum filler volume fractions. In this context, the optimum filler volume fractions are those for attaining the highest thermal contact conductance, as described in Section 3.2. In case of rough surfaces, although the GNP optimum volume fraction (2.4 vol.%) is much lower than the CB (Tokai) optimum volume fraction (15 vol.%), the GNP paste is more conductive thermally than the CB (Tokai) paste. In case of smooth surfaces, although the GNP optimum volume fraction (1.2 vol.%) is much lower than the CB (Tokai) optimum volume fraction (8 vol.%), the GNP paste is more conductive thermally than the CB (Tokai) paste. In spite of its high thermal

**Table 2 – Raw data in the thermal conductivity measurement of the paste with 2.4 vol.% GNP.**

Thickness ( $\mu\text{m}$ )	Thermal conductance ( $\times 10^4 \text{ W/m}^2 \text{ K}$ )	Thermal resistivity ( $\times 10^{-4} \text{ m}^2 \text{ K/W}$ )	Linear fit of the dependence of the thermal resistivity (y) on the bond line thickness (x) (Fig. 4)
50	0.905	1.105	$y = 2.103x + 6.2 \times 10^{-6} \text{ R}^2 = 0.999$
150	0.308	3.242	
200	0.235	4.251	



**Fig. 4 – Dependence of the thermal resistivity of the thermal contact on the thickness of the thermal paste. ( $\Delta$ ) 2.4 vol.% GNP; ( $\square$ ) 2.4 vol.% CB (Cabot); ( $\diamond$ ) 15 vol.% CB (Tokai). A vertical bar with a horizontal line at each end and indicating the data scatter is shown for each data point, though the bar is negligibly short for most data points.**

conductivity, the GNP paste at its optimum volume fraction gives thermal contact conductance that is comparable to the CB (Tokai) paste at its corresponding optimum volume fraction for the case of rough surfaces, and thermal contact conductance that is less than that for CB (Tokai) paste at its corresponding optimum volume fraction for the case of smooth surfaces (Table 1). At the respective optimum filler

volume fractions, whether the surfaces are rough or smooth, CB (Tokai) gives higher thermal conductivity than CB (Cabot) (Table 3). This explains the higher thermal contact conductance attained by CB (Tokai) at its optimum volume fraction than CB (Cabot) at its optimum volume fraction, whether the surfaces are rough or smooth, as shown in Table 1. At the same filler volume fraction, CB (Tokai) gives slightly higher thermal conductivity than CB (Cabot), although the difference is small. The above observations imply that, at the respective optimum filler volume fractions, (i) the high thermal conductivity of CB (Tokai) compared to CB (Cabot) is mainly due to the high value of the optimum filler volume fraction for CB (Tokai), and (ii) the high thermal conductivity of GNP compared to CB (Tokai) is due to the inherently high thermal conductivity of GNP.

In case of smooth surfaces and at the respective optimum filler volume fractions, the thermal contact conductance for the GNP paste (1.2 vol.%) is considerably lower than that for the CB (Tokai) paste (8 vol.%) and is slightly lower than that for the CB (Cabot) paste (2.4 vol.%) (Table 1). This occurs in spite of the relatively high thermal conductivity of the GNP paste (Table 3). This means that, at least for the case of smooth surfaces, the thermal conductivity is not a good indicator of the performance of a paste as a thermal interface material.

The highest thermal conductivity attained in this work for a GNP paste (4.8 vol.% GNP) is 0.75 W/mK, which is much lower than the value of 6.44 W/mK reported by Yu et al. [20] for a GNP epoxy-matrix composite (25 vol.% GNP). The relatively low thermal conductivity of this work is due to the low volume fraction of GNP.

**Table 3 – Thermal conductivity and geometric interfacial thermal resistivity of selected pastes under no load.**

Filler	Vol.%	Linear fit of the dependence of the thermal resistivity (y) on the bond line thickness (x) (Fig. 4)	Geometric interfacial resistivity <sup>a</sup> ( $\times 10^{-6} \text{ W/m}^2 \text{ K}$ )	Thermal conductivity (W/mK)
GNP	1.2	$y = 3.289x + 2.8 \times 10^{-5} \text{ R}^2 = 0.999$	$28 \pm 5$	$0.304 \pm 0.003$
	2.4	$y = 2.103x + 6.2 \times 10^{-6} \text{ R}^2 = 0.999$	$62 \pm 29$	$0.476 \pm 0.005$
	4.8	$y = 1.334x + 3.4 \times 10^{-5} \text{ R}^2 = 0.995$	$34 \pm 2$	$0.750 \pm 0.010$
CB (Tokai)	2.4	$y = 7.201x + 7.3 \times 10^{-6} \text{ R}^2 = 0.971$	$7.3 \pm 0.4$	$0.140 \pm 0.011$
	4.8	$y = 5.838x + 9.2 \times 10^{-6} \text{ R}^2 = 0.994$	$9.2 \pm 6.0$	$0.171 \pm 0.001$
	8.0	$y = 4.441x + 2.6 \times 10^{-5} \text{ R}^2 = 0.998$	$26 \pm 4$	$0.225 \pm 0.002$
	15.0	$y = 3.020x + 7.2 \times 10^{-6} \text{ R}^2 = 0.997$	$7.2 \pm 1.3$	$0.331 \pm 0.002$
CB (Cabot)	2.4	$y = 7.785x + 1.1 \times 10^{-5} \text{ R}^2 = 0.997$	$11 \pm 6$	$0.128 \pm 0.001$
	4.8	$y = 6.718x + 1.0 \times 10^{-5} \text{ R}^2 = 0.997$	$10 \pm 11$	$0.149 \pm 0.003$

<sup>a</sup>  $R_1A + R_2A$ , i.e., the total geometric interfacial resistivity.

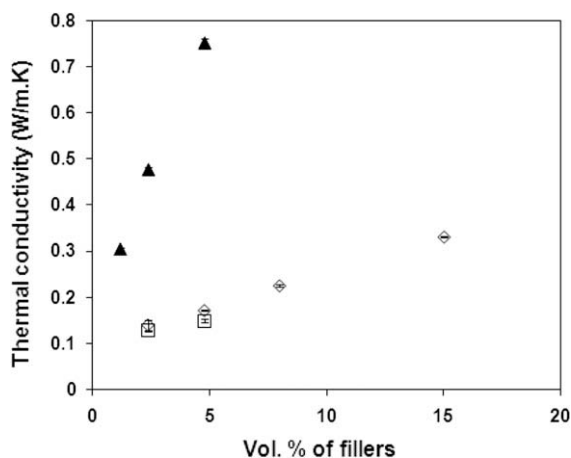


**Fig. 5 – Dependence of the thermal conductivity on the thickness for selected pastes. (▲) GNP pastes, (◇) Carbon black (Tokai), (□) carbon black (Cabot). A vertical bar with a horizontal line at each end and indicating the data scatter is shown for each data point, though the bar is negligibly short for most data points.**

### 3.4. Bond line thickness

An important factor that governs the performance of a thermal paste is the bond line thickness, which relates to the conformability and spreadability of the paste. According to Eq. (1), the thermal conductance, which is the inverse of the thermal resistivity, is related to the bond line thickness. A higher bond line thickness leads to a longer heat conduction path, and hence a higher thermal resistance.

Fig. 6 shows the change of the bond line thickness of GNP pastes with time from the start of application of a pressure of 780 Pa, as obtained by using Method B (Section 2.2.3). The thickness decreases abruptly at the start of loading, due to the partial squeezing out of the paste. The higher is the initial thickness, the greater is the amount squeezed out. The bond line thickness increases as the filler content increases. This

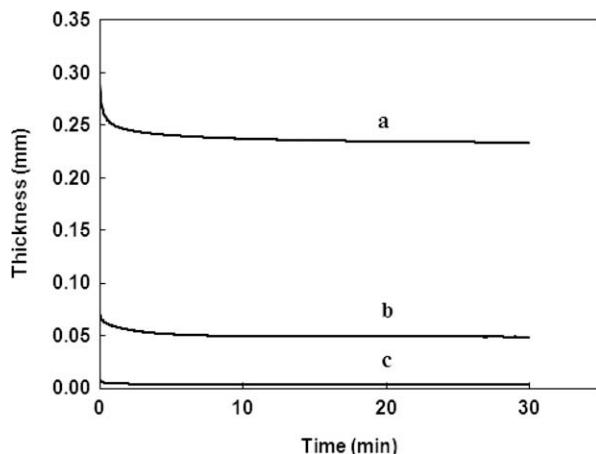


**Fig. 6 – Bond line thickness (measured using Method B) as a function of time from the start of application of a low compressive stress. (a) 1.2 vol.% GNP; (b) 2.4 vol.% GNP; (c) 4.8 vol.% GNP.**

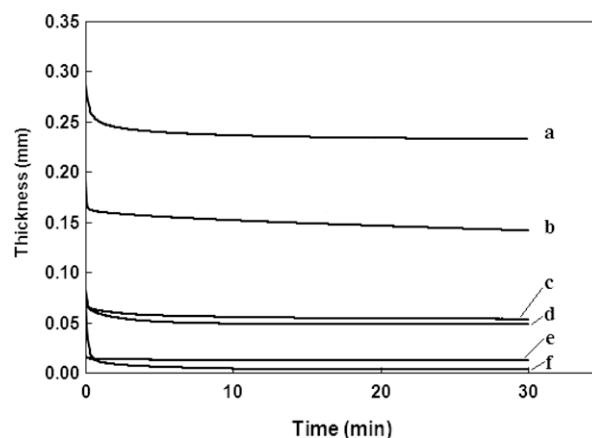
trend is expected, since the viscosity increases with the filler content. At the end of the period of loading, the thickness is 3, 49 and 230  $\mu\text{m}$  for GNP contents of 1.2, 2.4 and 4.8 vol.%, respectively.

As reported in Section 3.3, the thermal conductivity of the GNP paste increases as the filler content increases. However, a higher filler content leads to a larger bond line thickness, which increases the length of the heat conduction path, thereby decreasing the thermal conductance of the sandwich. Therefore, increasing the filler content to attain a higher thermal conductivity does not help, as the benefit due to the thermal conductivity increase is overshadowed by the negative effect of a higher bond line thickness.

The thickness in Fig. 6 was measured at 30 mN (780 Pa), whereas the thermal contact conductance testing was conducted at 0.46 MPa or above. Therefore, the bond line thickness in thermal contact conductance testing must be much smaller than the values in Fig. 6. Nevertheless, Fig. 6 is valuable for providing comparative information.

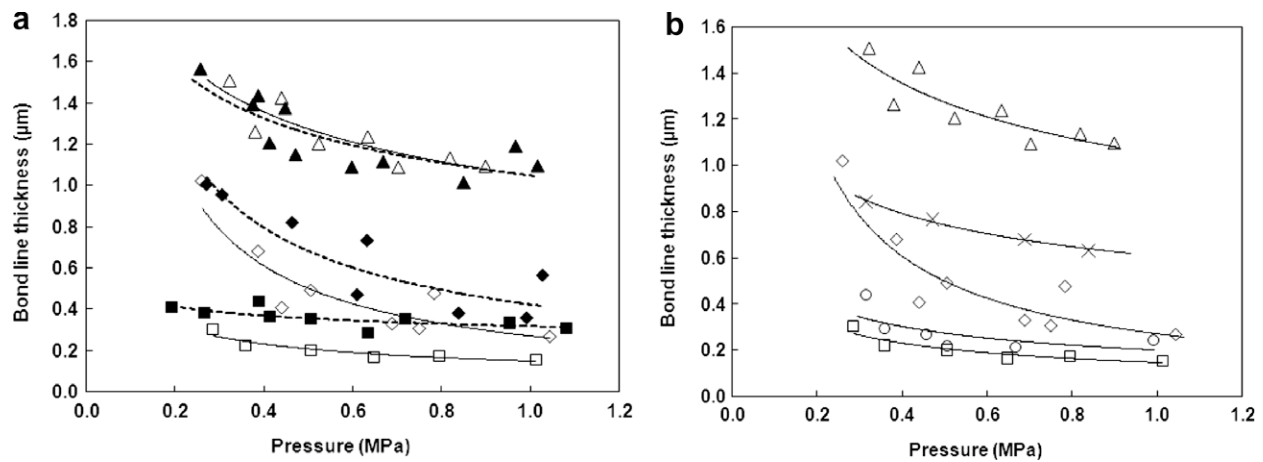
When compared with CB (whether Tokai or Cabot) at the same filler content, GNP gives higher bond line thickness, as shown in Fig. 7. The high bond line thickness is one of the causes for the low performance of the GNP paste compared to carbon black pastes. The performance is low in spite of the high thermal conductivity of the GNP paste compared to those of the carbon black pastes in the case of smooth surfaces (Section 3.2).

Fig. 8a and b show the dependence of the bond line thickness on pressure for various thermal pastes for rough and smooth proximate surfaces respectively, as obtained by using Method A (Section 2.2.3). For any paste, the bond line thickness decreases with increasing pressure, whether the proximate surfaces are rough or smooth. This trend is consistent with the increase in thermal contact conductance with increasing pressure, as observed for any of the pastes investigated, whether the proximate surfaces are rough or smooth (Table 1). This implies that the thermal contact conductance



**Fig. 7 – Bond line thickness (measured using Method B) as a function of time from the start of application of a low compressive stress. (a) 4.8 vol.% GNP paste; (b) 4.8 vol.% CB(Cabot) paste; (c) 4.8 vol.% CB(Tokai) paste; (d) 2.4 vol.% GNP paste; (e) 2.4 CB(Tokai) paste; (f) 2.4 vol.% CB (Cabot) paste.**





**Fig. 8 – Bond line thickness (measured using Method A) of various pastes. (a) Comparison of results for rough (solid symbols) and smooth (open symbols) proximate surfaces: (▲) 2.4 vol.% GNP pastes; (◆) 15 vol.% CB (Tokai); (■) 2.4 vol.% CB (Cabot). (b) Comparison of results of various pastes for smooth proximate surfaces: (Δ) 2.4 vol.% GNP pastes; (×) 1.2 vol.% GNP pastes; (◇) 15 vol.% CB (Tokai); (○) 8 vol.% CB (Tokai); (□) 2.4 vol.% CB (Cabot).**

correlates with the bond line thickness for any of the pastes investigated.

As shown in Fig. 8a, at the same pressure, 2.4 vol.% GNP gives the highest bond line thickness, 2.4 vol.% CB (Cabot) gives the lowest thickness and 15 vol.% CB (Tokai) gives an intermediate value, whether the proximate surfaces are rough or smooth. In particular, at a pressure of 0.46 MPa, which is one of the pressures used in the thermal contact conductance measurement, the bond line thickness is respectively 1.3, 0.72 and 0.36  $\mu\text{m}$  for 2.4 vol.% GNP, 15 vol.% CB (Tokai) and 2.4 vol.% CB (Cabot) pastes in case of rough surfaces.

Fig. 8b shows more complete data for the smooth case. At the same pressure and for the same type of filler, an increase in filler volume fraction increases the bond line thickness, as shown for GNP pastes (1.2 and 2.4 vol.%) and CB (Tokai) pastes (8 and 15 vol.%). This trend is expected.

Fig. 8b shows that, at the same pressure, the bond line thickness is lower for CB (Tokai) paste (8 vol.%, which is the optimum volume fraction for the smooth case, Table 1) than GNP paste (1.2 vol.%, which is the optimum volume fraction for the smooth case, Table 1). This explains why the former gives higher thermal contact conductance than the latter (Table 1). Fig. 8b shows that, at the same pressure, the bond line thickness is slightly lower for CB (Cabot) paste (2.4 vol.%, which is the optimum volume fraction for the smooth case, Table 1) than CB (Tokai) (8 vol.%, which is the optimum volume fraction for the smooth case, Table 1), but the former gives a lower value of the thermal contact conductance compared to the latter (Table 1). On the other hand, the former gives a lower value of the thermal conductivity than the latter (Table 3). These observations mean that the higher thermal contact conductance of CB (Tokai) paste (8 vol.%) compared to CB (Cabot) (2.4 vol.%) is due to its higher thermal conductivity, which overshadows the negative effect of the larger bond line thickness of CB (Tokai) paste (8 vol.%).

Fig. 8 shows that the bond line thickness varies with the pressure more significantly for CB (Tokai) paste (15 vol.%) than any of the other pastes, which include the CB (Tokai)

paste (8 vol.%) shown in Fig. 8b. The more significant pressure dependence of CB (Tokai) paste (15 vol.%) is attributed to its high filler volume fraction, which causes the minimum pressure for substantial decrease of the bond line thickness to be relatively high.

For the same CB paste (whether Tokai or Cabot), the bond line thickness is lower for the smooth surfaces than the rough surfaces. For the GNP paste, the bond line thickness is essentially the same for smooth and rough surfaces. This difference between CB and GNP pastes may be because of the greater difficulty for the GNP paste to be compressed into the microscopic valleys in the proximate surfaces (due to the GNP nanoplatelets being large compared to the CB nanoparticles) and the consequent low conformability of the GNP paste compared to the CB pastes.

Due to the low bond line thickness for the smooth case compared to the rough case for the CB pastes and the absence of effect of proximate surface roughness on the bond line thickness for the GNP paste, the difference in bond line thickness between the GNP paste and any of the CB pastes is larger for the smooth case than the rough case. This explains why the thermal contact conductance is lower for the GNP paste than the CB (Tokai) paste in the smooth case, but is comparable for these pastes in the rough case (Fig. 3).

For any of the pastes, the thermal contact conductance is higher for the smooth case than the rough case (Table 1). In the case of the CB pastes, this is at least partly due to the lower value of the bond line thickness for the smooth case. In the case of the GNP paste, this explanation does not work, since the bond line thickness is the same for the smooth and rough cases. Therefore, the explanation for the GNP paste probably relates to the lower geometric interfacial resistivity for the smooth case, though evidence is not available to support this explanation.

Although the bond line thickness for the 8 vol.% CB (Tokai) paste is not included in Fig. 8 for the sake of presentation clarity, its value, as measured for the smooth case, is lower than that for the 15 vol.% CB (Tokai) paste and is close to that for

the 2.4 vol.% CB (Cabot) paste. This means that, at the same pressure and for the same filler, the bond line thickness is larger when the filler volume fraction is higher, as expected.

#### 4. Conclusion

Comparative evaluation of GNP, CB (Tokai) and CB (Cabot) pastes in their effectiveness as thermal interface materials between copper proximate surfaces of roughness 15  $\mu\text{m}$  and held together at pressures ranging from 0.46 to 0.92 MPa shows that the optimum filler volume fraction for attaining the maximum thermal contact conductance are 2.4, 15 and 2.4 vol.% for GNP, CB (Tokai) and CB (Cabot) respectively. Except for CB (Cabot), the optimum filler volume fraction is diminished when the roughness is decreased from 15 to 0.009  $\mu\text{m}$ ; it is diminished from 2.4 to 1.2 vol.% for GNP and from 15 to 8 vol.% for CB (Tokai). Comparing the fillers at their respective optimum volume fractions shows that (i) GNP is comparable in effectiveness to CB (Tokai) for rough (15  $\mu\text{m}$ ) surfaces, but is less effective than CB (Tokai) for smooth (0.009  $\mu\text{m}$ ) surfaces, and (ii) GNP is more effective than CB (Cabot) for rough surfaces, but is slightly less effective than CB (Cabot) for smooth surfaces. With consideration of the material cost, the processing complexity, the chemical reactivity (with likely residual acid in GNP) and the thermal contact conductance, CB is a much more attractive choice than GNP as a filler for thermal pastes.

Measurement of the thermal conductivity within a paste under no pressure shows that, GNP gives higher thermal conductivity than either type of CB, whether the comparison is at the same filler volume fraction or at the respective optimum filler volume fractions. In spite of its high thermal conductivity, the GNP paste at its optimum volume fraction gives thermal contact conductance that is comparable to the CB (Tokai) paste at its corresponding optimum volume fraction in case of rough surfaces, and thermal contact conductance that is lower than that of CB (Tokai) paste at its corresponding optimum volume fraction in case of smooth surfaces. At the respective optimum filler volume fractions, whether the surfaces are rough or smooth, CB (Tokai) gives higher thermal conductivity than CB (Cabot). This explains the higher thermal contact conductance attained by CB (Tokai) than CB (Cabot) at their respective optimum volume fractions for both rough and smooth cases. At the same filler volume fraction, GNP gives higher thermal conductivity than CB (Tokai or Cabot), while CB (Tokai) gives slightly higher thermal conductivity than CB (Cabot).

The bond line thickness decreases with increasing pressure, such that the effect is more significant for CB (Tokai) paste (15 vol.%) than any of the other pastes studied. This is due to the high filler volume fraction of this paste.

At the same pressure, GNP gives higher bond line thickness than CB (Tokai or Cabot), whether at the same filler volume fraction or at the respective optimum filler volume fractions (whether the surfaces are rough or smooth). Thus, in spite of the high thermal conductivity of GNP, the effectiveness of GNP is limited, due to the high bond line thickness.

At the same pressure, CB (Tokai) gives higher bond line thickness than CB (Cabot), whether at the same filler volume

fraction or at the respective optimum filler volume fraction (whether the surfaces are rough or smooth), although the difference is small in case of comparison at the same filler volume fraction of 2.4 vol.% and in case of comparison at the corresponding optimum filler volume fractions for the smooth case. The superior thermal contact conductance of CB (Tokai) compared to CB (Cabot) is attributed to the higher thermal conductivity, which overshadows the effect of the larger bond line thickness.

All values of the thermal contact conductance reported in this work are higher than the highest value of  $8 \times 10^3 \text{ W/m}^2\text{K}$  that had been previously reported for an aligned multiwalled carbon nanotube (0.4 vol.%) array [23]. Though the thermal conductivity of the array is 1.21 W/mK, which is higher than any of the thermal conductivity values of the pastes of this work, the array's high bond line thickness (0.1 mm or above) limits its effectiveness.

In general, in order to attain high performance, as indicated by the thermal contact conductance of the sandwich, high thermal conductivity, small bond line thickness and low geometric interfacial resistivity are valuable. High thermal conductivity alone does not necessarily mean high thermal contact conductance. In particular, for a paste that is relatively low in the thermal conductivity (e.g., a carbon black paste), a sufficiently low value of the bond line thickness can cause the paste to be highly effective.

#### REFERENCES

- [1] Chung DDL. Advances in thermal interface materials. *Advancing Microelectronics* 2006;33(4):8–11.
- [2] Leong C-K, Chung DDL. Carbon black dispersions as thermal pastes that surpass solder in providing high thermal contact conductance. *Carbon* 2003;41(13):2459–69.
- [3] Leong C-K, Chung DDL. Carbon black dispersions and carbon-silver combinations as thermal pastes that surpass commercial silver and ceramic pastes in providing high thermal contact conductance. *Carbon* 2004;42(11):2323–7.
- [4] Leong C-K, Aoyagi Y, Chung DDL. Carbon-black thixotropic thermal pastes for improving thermal contacts. *J Electron Mater* 2005;34(10):1336–41.
- [5] Leong C-K, Aoyagi Y, Chung DDL. Carbon black pastes as coatings for improving thermal gap-filling materials. *Carbon* 2006;44(3):435–40.
- [6] Howe TA, Leong C-K, Chung DDL. Comparative evaluation of thermal interface materials for improving the thermal contact between an operating computer microprocessor and its heat sink. *J Electron Mater* 2006;35(8):1628–35.
- [7] Lin C, Howe TA, Chung DDL. Electrically nonconductive thermal pastes with carbon as the thermally conductive component. *J Electron Mater* 2007;36(6):659–68.
- [8] Aoyagi Y, Chung DDL. Effects of antioxidants and the solid component on the thermal stability of polyol-ester-based thermal pastes. *J Mater Sci* 2007;42(7):2358–75.
- [9] Xu Y, Leong C-K, Chung DDL. Carbon nanotube dispersions as thermal pastes. *J Electron Mater* 2007;36(9):1181–7.
- [10] Anderson SH, Chung DDL. Exfoliation of intercalated graphite. *Carbon* 1984;22(3):253–63.
- [11] Viculis LM, Mack JJ, Mayer OM, Hahn HT, Kaner RB. Intercalation and exfoliation routes to graphite nanoplatelets. *J Mater Chem* 2005;15(9):974–8.

- [12] Cho J, Chen JY, Daniel IM. Mechanical enhancement of carbon fiber/epoxy composites by graphite nanoplatelet reinforcement. *Scripta Met* 2007;56(8):685–8.
- [13] Adegard GM, Gates TS. Modeling and testing of the viscoelastic properties of a graphite nanoplatelet/epoxy composite. *J Intell Mater Syst Struct* 2006;17(3):239–46.
- [14] Kalaitzidou K, Fukushima H, Drzal LT. Processing, properties and structure of exfoliated graphite nanoplatelet-polypropylene nanocomposites. In: *AlChE annual meeting, conference proceedings*, Cincinnati, OH, 2005, American Institute of Chemical Engineers, New York, NY, 2005. p. 128e/1–19.
- [15] Kalaitzidou K, Fukushima H, Drzal LT. Mechanical properties and morphological characterization of exfoliated graphite-polypropylene nanocomposites. *Compos: Part A* 2007;38:1675–82.
- [16] Li J, Kim J-K. Percolation threshold of conducting polymer composites containing 3D randomly distributed graphite nanoplatelets. *Compos Sci Tech* 2007;67(10):2114–20.
- [17] Li J, Sham ML, Kim J-K, Marom G. Morphology and properties of UV/ozone treated graphite nanoplatelet/epoxy nanocomposites. *Compos Sci Tech* 2007;67(2):296–305.
- [18] Fukushima H, Drzal, LT. Nylon-exfoliated graphite nanoplatelet (xGnP) nanocomposites with enhanced mechanical, electrical and thermal properties. *NSTI Nanotech 2006, NSTI Nanotechnology Conference and Trade Show*, Boston, MA, 2006, vol. 1, Nano Science and Technology Institute, Cambridge, MA, p. 282–5.
- [19] Hung MT, Choi O, Ju YS, Hahn HT. Heat conduction in graphite-nanoplatelet-reinforced polymer nanocomposites. *Appl Phys Lett* 2006;89(2):023117/1–3.
- [20] Yu A, Ramesh P, Itkis ME, Bekyarova E, Haddon RC. Graphite nanoplatelet-epoxy composite thermal interface materials. *J Phys Chem C* 2007;111(21):7565–9.
- [21] Luo X, Chugh R, Biller B C, Hoi YM, Chung DDL. Electronic applications of flexible graphite. *J Electron Mater* 2002;31(5):535–44.
- [22] Borca-Tasciuc T, Mazumder M, Son Y, Pal SK, Schadler LS, Ajayan PM. Anisotropic thermal diffusivity characterization of aligned carbon nanotube-polymer composites. *J Nanosci Tech* 2007;7(4–5):1581–8.
- [23] Huang H, Liu C, Wu Y, Fan S. Aligned carbon nanotube composite films for thermal management. *Adv Mater* 2005;17:1652–6.
- [24] Xu Y, Chung DDL. Increasing the thermal conductivity of boron nitride and aluminum nitride particle epoxy-matrix composites by particle surface treatment. *Compos Interf* 2000;7(4):243–56.
- [25] Chiu CP, Solbrekken GL, Chung YD. Thermal modeling of grease-type interface material in PPGA application. In: *Proceedings of the 13th IEEE Semi-Therm*, vol. 1, 1997. p. 57–63.
- [26] Prasher R, Koning P, Shipley J, Devpura A. Dependence of thermal conductivity and mechanical rigidity of particle-laden polymeric thermal interface material on particle volume fraction. *J. Electron Packag* 2003;125:386–91.
- [27] Lin C, Chung DDL. Effect of carbon black structure on the effectiveness of carbon black thermal interface pastes. *Carbon* 2007;45(15):2922–31.
- [28] *Perkin-Elmer Users Manual*, 7 Series/UNIX TMA 7, Perkin-Elmer Corp., Norwalk, CT, 1992.
- [29] Debelak B, Lafdi K. Use of exfoliated graphite filler to enhance polymer physical properties. *Carbon* 2007;45:1727–34.